JACS
JOURNAL OF THE AMERICAN CHEMICAL SOCIETY
Article
pubs.acs.org/JACS

SSZ-52, a Zeolite with an 18-Layer Aluminosilicate Framework Structure Related to That of the DeNOx Catalyst Cu-SSZ-13

Dan Xie,[†,‡] Lynne B. McCusker,*[,‡] Christian Baerlocher,[‡] Stacey I. Zones,*[,†] Wei Wan,[§] and Xiaodong Zou[§]

[†]Chevron Energy Technology Company, Richmond, California 94802, United States

[‡]Laboratory of Crystallography, ETH Zurich, CH-8093 Zurich, Switzerland

[§]Berzelii Center EXSELENT on Porous Materials, Department of Materials and Environmental Chemistry, Stockholm University, SE-106 91 Stockholm, Sweden

Supporting Information

ABSTRACT: A new zeolite (SSZ-52, $|(C_{14}H_{28}N)_6Na_6(H_2O)_{18}|[Al_{12}Si_{96}O_{216}]$), related to the DeNOx catalyst Cu-SSZ-13 (**CHA** framework type), has been synthesized using an unusual polycyclic quaternary ammonium cation as the structure-directing agent. By combining X-ray powder diffraction (XPD), high-resolution transmission electron microscopy (HRTEM) and molecular modeling techniques, its porous aluminosilicate framework structure ($R\bar{3}m$, a = 13.6373(1) Å, c = 44.7311(4) Å), which can be viewed as an 18-layer stacking sequence of hexagonally arranged $(Si,Al)_6O_6$ rings (6-rings), has been elucidated. The structure has a three-dimensional 8-ring channel system and is a member of the ABC-6 family of zeolites (those that can be described in terms of 6-ring stacking sequences) like SSZ-13, but it has cavities that are twice as large. The code SFW has been assigned to this new framework type. The large cavities contain pairs of the bulky organic cations. HRTEM and XPD simulations show that stacking faults do occur, but only at the 5−10% level. SSZ-52 has considerable potential as a catalyst in the areas of gas conversion and sequestration.

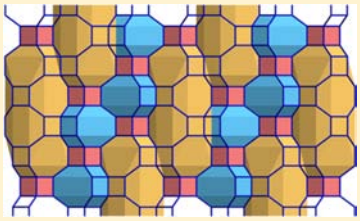

1. INTRODUCTION

Recently, there has been a surge of activity in the zeolite technology area with the commercialization of the copper-SSZ-13 zeolite (**CHA** framework type[1,2]) as a DeNOx catalyst for emission control in trucks.[3−6] Efforts to understand this catalyst system have focused on the siting of the copper near the double 6-ring (*d6r*) building units that cap the *cha* cavities[7] in the **CHA** framework. SSZ-13 belongs to the ABC-6 family of framework structures, which are composed of layers of hexagonally arranged 6-rings stacked in different sequences.[8] As in the packing of spheres, there are three possible positions for the lateral translation of the layers, denoted as A, B, and C, and the **CHA** framework type is characterized by the stacking sequence AABBCC. Recent work on the zeolites SSZ-16[6b] (framework type **AFX**, stacking sequence AABBCCBB), SSZ-39[9] (framework type **AEI**, not a member of the ABC-6 family, but closely related to **CHA**) and SSZ-17[10] (framework type **LEV**, stacking sequence AABCCABBC) seems to indicate that other members of the ABC-6 family with *d6r* units might also provide a good environment for the Cu DeNOx catalytic reaction.

About a decade ago, Gregory S. Lee at Chevron, focused efforts on creating novel, structure-directing agents (SDAs) using Michael addition chemistry. This is a good entry into the creation of rigid polycyclic compounds, which can be used as SDAs in zeolite synthesis. SDAs are the guest organic cations around which the host zeolite framework can form, and their incorporation into a zeolite synthesis can lead to novel high-silica architectures (e.g., SSZ-50 (**RTH**)),[11] where the organic guest fills the void space of the zeolite. This strategy led to the creation of the SDA shown in Figure 1[12] (full reaction scheme shown in Figure S1 in Supporting Information [SI]). By using this novel cyclohydrocarbon as an SDA, and tuning the zeolite synthesis conditions appropriately, we attempted to create a new zeolite framework structure.

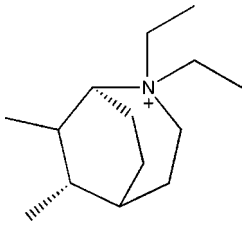

Figure 1. Polycyclic structure-directing agent used to produce the zeolite SSZ-52.

Our general approach, once an SDA has been created, is to screen it in zeolite syntheses where a range of inorganic ratios are used. This gives rise to the possibility of different types of subunits (smaller rings) being created in the different syntheses. For products based upon alumino, germano, boro, and fluorosilicates, the zeolite host is created as these subunits connect in an ordered manner. The modification of OH/Si or

Received: May 2, 2013
Published: June 19, 2013

   dx.doi.org/10.1021/ja4043615 | J. Am. Chem. Soc. 2013, 135, 10519−10524

F/Si ratios[13] and the incorporation of certain elements can bias the likelihood that particular subunits form.[14] Lower OH/Si and higher Si/Al ratios, for example, favor products rich in 5-rings.

With the new SDA shown in Figure 1, only under high OH/Si conditions was a novel zeolite structure produced, and the material proved to be relatively rich in Al. Zeolites such as SSZ-13, -16, and -17 (*vide supra*) crystallize under similar conditions. All of these zeolites are members of the ABC-6 family, which contain 4- and 6- but not 5-rings, so we were excited to consider that the new zeolite, SSZ-52,[13] might also be a member of this family. Indeed, micropore volume measurements indicated that the internal void space was very high for this material once the SDA had been removed by calcination. Acid-catalyzed conversion of methanol yielded mainly C2−C4 olefins, as had been observed for zeolites like SSZ-13, which is indicative of a large cavity with small pore (8-ring) access. Both of these features are consistent with the behavior of the other members of the ABC-6 family of zeolites mentioned earlier.

We describe here the solution of the structure of this novel zeolite, which is indeed a member of the ABC-6 family and has the largest cavity ever made in this family. The very sizable cavity of SSZ-52 is filled with not one, but two, of the bulky organocations, a most unusual phenomenon. By applying multiple structural characterization techniques, we have been able to understand the finer details of the structure, including a quantification of the stacking faults, and to postulate a growth mechanism for the framework structure. The potential of SSZ-52 for application in DeNOx catalysis or as an adsorbent in areas like CO_2 capture,[15] is exciting.

2. STRUCTURE DETERMINATION

Like most synthetic zeolites, SSZ-52 is polycrystalline. High-resolution X-ray powder diffraction (XPD) data were collected on a sample of as-made SSZ-52 using the powder diffractometer on the Swiss-Norwegian Beamlines (SNBL) at the European Synchrotron Radiation Facility (ESRF) in Grenoble, France. The combination of sharp and broad peaks in the XPD pattern is indicative of an extreme morphology such as thin plates or long needles and/or disorder in a particular direction, and initial attempts to index the pattern using standard automatic indexing algorithms failed. As it was suspected that SSZ-52 might be a member of the ABC-6 family, the lattice parameters of existing family members were examined. All 19 ABC-6 structures found in the Zeolite Structure Database[2] can be indexed using a hexagonal lattice with a (or b) in the range of 13 ± 1 Å. The c axis varies, depending on the ABC stacking sequence. On average, a layer has a thickness of ~2.5 Å. With this information, it was possible to identify a two-dimensional (2D) hexagonal unit cell ($a = b =$ 13.637 Å) using only the sharp peaks in the XPD pattern. From the broader peaks, it was then possible to determine the length of the c axis (~44.73 Å), and the number of 6-ring layers (44.73 Å/2.5 Å ≈ 18). Only reflections with $-h + k + l = 3n$ were observed in the powder diffraction pattern, so a rhombohedral centering was expected. Further examination of the lattice parameters within the ABC-6 family revealed that the lengths of their a axes are very sensitive to the number of *d6r* layers in the stacking sequence (Table 1).

The a axis of SSZ-52 had been determined to be 13.637 Å, so this was taken as a strong indication that the framework would consist of *d6r* layers only. A systematic enumeration of all possible 9-layer *d6r* stacking sequences yielded a total of seven unique solutions (Table 2). For simplicity, the notation AA = 𝔸, BB = 𝔹 and CC = ℂ is used in the table and the rest of the text.

Table 1. Correlation between the Layer Structure and the *a*-Axis for the ABC-6 Family of Zeolites

layer structure	a (Å)
double 6-rings only	13.65−13.75
double and single 6-rings	12.85−13.20
single 6-rings only	12.25−12.70

Table 2. Seven Possible 9-Layer *d6r* Stacking Sequences

model number	stacking sequence	ideal space group
1	𝔸B𝔸BℂBℂ𝔸ℂ	$R\bar{3}m$
2	𝔸BℂBℂBℂBℂ	$P\bar{3}m1$
3	𝔸BℂBℂBℂ𝔸B	$P3m1$
4	𝔸BℂBℂB𝔸BC	$P3m1$
5	𝔸BℂBℂ𝔸BℂB	$P3m1$
6	𝔸BℂB𝔸ℂB𝔸ℂ	$P\bar{3}m1$
7	𝔸BℂBℂ𝔸B𝔸ℂ	$P\bar{3}m1$

Only model 1 is consistent with the rhombohedral centering observed in the powder diffraction pattern. Nonetheless, the geometry of each model was optimized using the distance-least-squares program DLS-76[16] assuming the unit cell dimensions found for SSZ-52. A comparison between the XPD pattern calculated for each of the seven models and the measured one shows quite clearly that model 1, with the highest symmetry ($R\bar{3}m$), gives the best match (Figure S2 in SI). This model was then used as a starting point for the Rietveld refinement of the structure.

Difference electron density maps showed a cloud of electron density in the large cavity, but the individual atoms of the SDA could not be resolved, so molecular modeling was used to get an initial estimate of their positions. Interaction energy optimization was carried out with the Materials Studio software[17] by docking first one SDA in the large cavity and then increasing the number until the lowest interaction energy was found (see SI for details). The energy-optimized configuration with two SDAs in the large cavity was then used to continue the structure refinement. Further difference electron density maps revealed the locations of other nonframework species (1 Na and 3 H_2O per *gme*[7] cavity). Rietveld refinement with geometric restraints imposed on the bond distances and angles of the atoms in both the framework and the SDA, proceeded smoothly and converged with R_F = 0.059 and R_{wp} = 0.217 (R_{exp} = 0.117). The high profile R_{wp}-value is related to the fact that the different peak shapes are difficult to describe accurately, but the R_F value clearly indicates that the structure is basically correct. The framework structure showing the arrangement of the different types of cages/cavities in the structure, the location of the two bulky organic cations in the large cavity, and the profile fit for the Rietveld refinement are presented in Figure 2a,b,c, respectively. Crystallographic details are given in Table 3.

The ideal framework structure of SSZ-52 (SFW) can be built by arranging blocks of *d6r*−*gme*−*d6r*−*gme*−*d6r* building units[7] in a rhombohedral manner. This arrangement leads to the formation of a new large cavity between the blocks (ten 6-ring layers, see Figure 2a). These large cavities are connected to each other laterally via 8-ring windows. The only other

dx.doi.org/10.1021/ja4043615 | J. Am. Chem. Soc. 2013, 135, 10519−10524

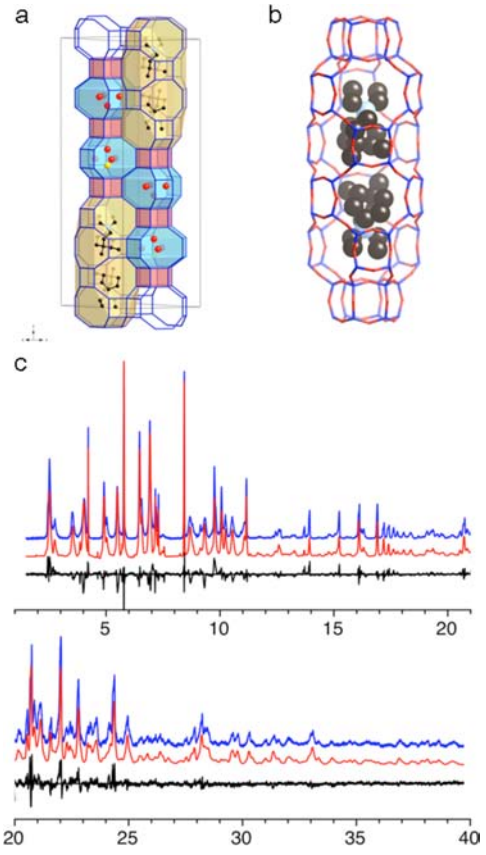

Figure 2. Refined structure of SSZ-52. (a) Framework structure showing the three different types of cages/cavities (pink: *d6r*; blue: *gme*; yellow: large cavity) and the locations of the nonframework species (blue: Si,Al; red: O (water); yellow: Na; black: C; light blue: N). Framework O atoms have been omitted for clarity. (b) The arrangement of the two SDA molecules in the large cavity. (c) The observed (blue), calculated (red), and difference (black) profiles for the Rietveld refinement of the structure shown in (a). The second half of the pattern has been scaled up by a factor of 5 to show more detail.

Table 3. Crystallographic Data for SSZ-52

synchrotron facility	SNBL (station B) at ESRF
wavelength	0.501171(4) Å
sample	1 mm capillary
2θ range (deg)	0.4–45.5° 2θ
step size (deg)	0.004° 2θ
chemical composition	$\vert(C_{14}H_{28}N)_6Na_6(H_2O)_{18}\vert[Al_{12}Si_{96}O_{216}]$
a (Å)	13.6373(1)
c (Å)	44.7311(4)
space group	$R\bar{3}m$
number of observations	9506
contributing reflections	2087
geometric restraints	174
positional parameters	138
framework	29
C	39
N	1
H	64
Na	3
water	2
R_F	0.059
R_{wp}	0.217
R_{exp}	0.117

members of the ABC-6 family of zeolite structures that can be built entirely from *d6r* layers are **CHA**, **GME**, **AFT**, and **AFX**. The **GME** framework (𝔸𝔹) has no ℂ layer, so it has a 1D 12-ring channel system with no 8-ring connections between the channels, and the **AFT** framework has only been synthesized in the aluminophosphate system. A comparison of SSZ-52 with the two remaining framework structures and their cavities is shown in Figure S3 in SI. All three can be described in terms of a *d6r* stacking sequence, have 3D 8-ring channel systems, and can be made in aluminosilicate form. The difference lies in the size of the cavities within the channel system.

3. ELECTRON MICROSCOPY

In an attempt to gain some insight into the degree of disorder in SSZ-52, we further investigated the SSZ-52 sample by SAED and HRTEM. The SAED pattern in Figure 3a was taken along

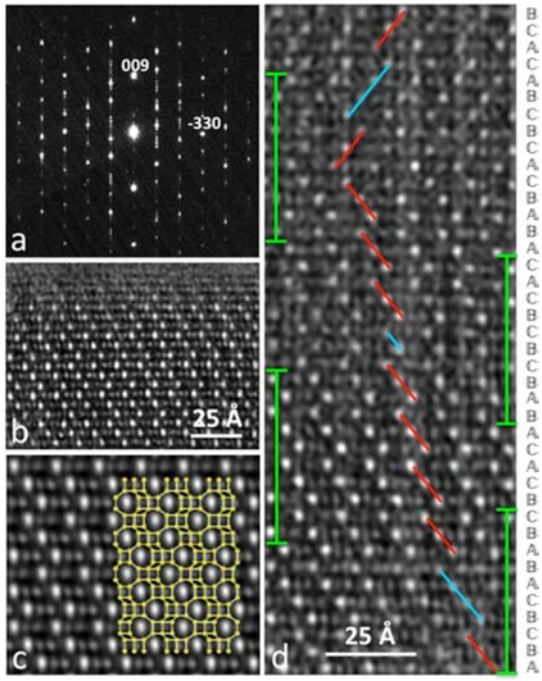

Figure 3. SAED pattern and HRTEM images of the [100] projection of SSZ-52. (a) SAED pattern showing streaks along the c^* direction, which indicates stacking disorder. (b) The projection of an ordered part of a crystal. (c) Averaged image ($p1$) from (b) with the structure overlaid. (d) [100] projection taken from a disordered part of an SSZ-52 crystal with a schematic description of the stacking disorder overlaid. The stacking sequence of the *d6r* layers is given on the right. Green bars mark the regions reproduced in Figure 6. Each HRTEM image was averaged from 20 HRTEM images taken under identical conditions in order to enhance the signal-to-noise ratio.

the [100] projection. It shows streaks along the [001] direction, indicating the presence of stacking disorder in the SSZ-52 crystals. The HRTEM image in Figure 3b was taken from a defect-free region of an SSZ-52 crystal and is clearly consistent with the refined framework model (Figure 3c). With a stacking sequence of *d6r* layers, only 8-ring pores are formed in this direction (single 6-ring layers generate 6-rings). Images taken along other projections show a similar agreement with the framework model (Figure S4 in SI). In addition, electron diffraction patterns simulated from the refined structure agree with the corresponding SAED patterns (Figure S5 in SI).

dx.doi.org/10.1021/ja4043615 | J. Am. Chem. Soc. 2013, 135, 10519–10524

However, other HRTEM images highlight the presence of some stacking disorder, as shown in Figure 3d and Figure S6 in SI. The sequence of three sets of three *d6r*-layer blocks in SSZ-52 (i.e., the *d6r*-layer repeat sequence (𝔸𝔹ℂ 𝔹ℂ𝔸 ℂ𝔸𝔹) is occasionally disturbed and sometimes the stacking reverses direction (twinning).

4. DIFFAX SIMULATIONS

A simulation of the XPD pattern using the DIFFaX algorithm[18] was performed in an attempt to quantify the degree of disorder. The ideal framework structure can be simulated with DIFFaX by using a single 𝔸𝔹ℂ three-*d6r* block combined with rhombohedral centering translations. In the real structure, however, additional blocks (e.g., 𝔸𝔹ℂ𝔸 four-*d6r* block and 𝔸𝔹 two-*d6r* block) are also present as a result of stacking faults. By adjusting the stacking probabilities of different blocks, an excellent match between the simulated and experimental XPD patterns could be obtained with 8% stacking faults, 2% of which cause twinning (Figure 4). For all simulations, the pseudo-Voigt peak profile parameters (u, v, w, δ) used in DIFFaX were 0.078, 0.0002, 0.0002, and 0.6, respectively.

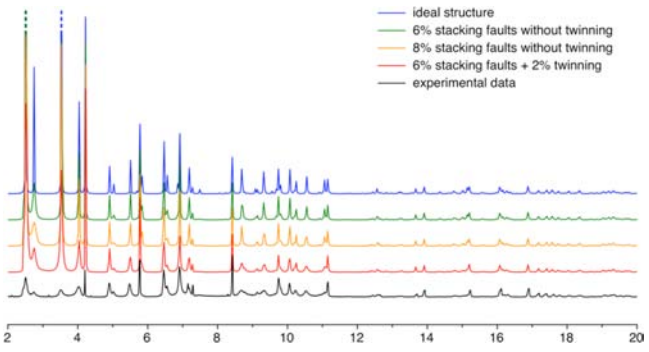

Figure 4. Comparison of the experimental XPD pattern for SSZ-52 (black) with those simulated with DIFFaX for the ideal framework structure (blue), for the ideal framework structure with 6% (green) and 8% (orange) stacking faults of the kinds shown in Figure 6c,d, and for the ideal framework structure with 6% stacking faults of the kinds shown in Figure 6c,d and 2% of the twinning stacking faults shown in Figure 6e,f (red). It should be noted that the differences in the intensities in the low 2θ region are due to the presence of extra-framework species in the structure (e.g., SDA molecules, water molecules, Na^+ ions) that were not included in the DIFFaX simulation.

5. DISCUSSION

One of the more unusual features of the SSZ-52 structure is the presence of two SDAs in a single cavity. Indeed, this is the only instance we are aware of in which a zeolite cavity is filled and stabilized by two such bulky organic cations. In their synthesis of ITQ-29, a pure silica form of the **LTA**-type zeolite, Corma and co-workers used a large aromatic SDA that was known to form pairs via $\pi-\pi$-type interactions,[19] but they only characterized the structure of the calcined material in which the SDA had been removed. Nonetheless, the assumption that pairs of the organic cation acted as a structure-directing agent in that case is a reasonable one, because the intermolecular forces involved are quite strong. However, in the case of SSZ-52, the organic cations can only interact with one another via van der Waals-type forces, and thus, a pairing was not anticipated.

A careful examination of the structure reveals that the pairs of cations in SSZ-52 probably direct not only the size of the large cavities but also their rhombohedral arrangement. Both the refined structure and energy calculations indicate that the paired arrangement of the SDAs in the large cavity as shown in Figure 2b is the preferred one. One can imagine a crystal growth sequence (see Table 4 and Figure 5) in which two *d6r*

Table 4. Crystal Growth Sequence Showing the Occupancies of the Three Different Positions in Each of the Nine *d6r* Layers[a]

layer	position A	position B	position C
9	*gme*	*d6r*	SDA1
8	*d6r*	$SDA2^+$	$SDA1^+$
7	*gme*	SDA2	*d6r*
6	*d6r*	SDA1	*gme*
5	$SDA2^+$	$SDA1^+$	*d6r*
4	SDA2	*d6r*	*gme*
3	SDA1	*gme*	*d6r*
2	$SDA1^+$	*d6r*	$SDA2^+$
1	*d6r*	*gme*	SDA2

[a]Each SDA fills two *d6r* layers, the positive end of the SDA is indicated with a + sign.

layers (positions A and B) connect to form a hole (position C) and a cup (position A). In the cup, the positive end of the SDA fits well to balance the charge of the anionic framework. The subsequent stacking of the *d6r* units is dictated by the position adopted by the SDA and the position of the previous layer of *d6r* units. In the third layer, for example, the *d6r* units can only position themselves above the hole, because they cannot be directly above the *d6r* units in position B and the less positive part of the SDA occupies position A. In fact, the hole would not be empty but would contain the positive end of an SDA from previous layers. In the fourth layer, a second SDA positions itself above the previous one (position A) with its positive end pointed in the other direction. Apparently this pairing arrangement in position A is energetically favored over the cup that is formed in position B, so the *d6r* unit occupies that position and forms a *gme* cavity. This preference may also be influenced by the presence of Na^+ ions, which were found to fill the *gme* cavities. In the fifth layer, the second SDA is in position A, so the *d6r* must adopt position C. This creates a cup in position B for the next SDA and the sequence begins again. In the sixth layer, the *d6r* unit in position A forms an inverted cup over the inverted SDA. The second pair of SDAs is related to the first pair via a rhombohedral translation ($x + 2/3$, $y + 1/3$, $z + 1/3$). It is reasonable to assume that the negative charge of the framework, created by the presence of Al^{III} in place of Si^{IV}, is concentrated near the positive end of the SDA and the Na^+ ions, but the exact location of Al could not be determined in this study.

Given the ideal growth sequence described above, it is easy to see that "mistakes" can happen (Figure 6). However, the HRTEM images show that there are only two types of stacking faults present (apart from twinning), and this is confirmed by the DIFFaX simulations. The proposed growth mechanism would explain how subtle changes in the templating action of the SDA might result in stacking faults. A *d6r* can cap a cavity with only one SDA in it to form a *cha* cavity instead of the longer SSZ-52 cavity (Figure 6c), or a third SDA cation can position itself above an existing pair instead of in the neighboring cup to form an even longer cavity (Figure 6d). Thus, the SDA positioning explains not only the normal growth

dx.doi.org/10.1021/ja4043615 | J. Am. Chem. Soc. 2013, 135, 10519−10524

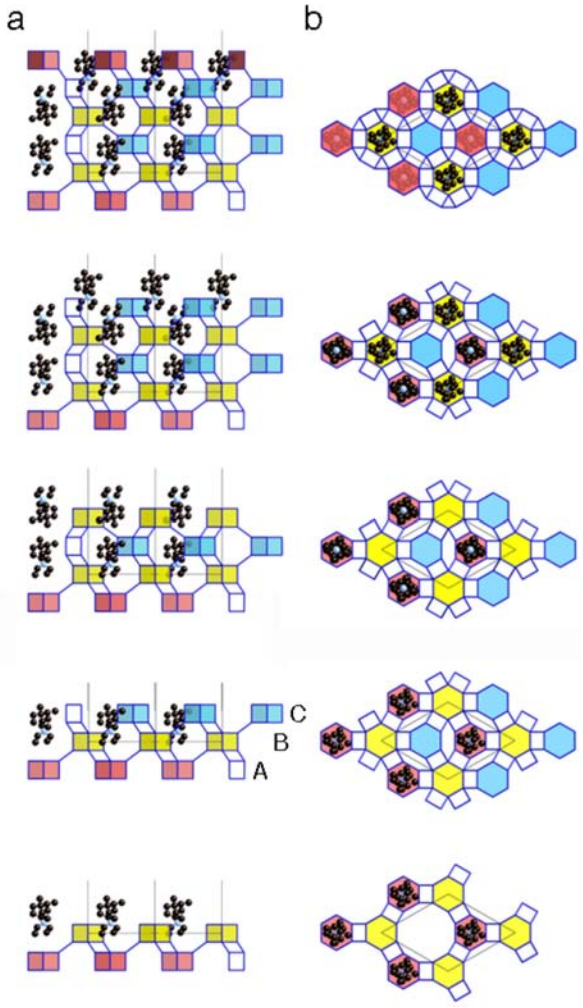

Figure 5. The *d6r* stacking in SSZ-52 and its relationship to the position of the SDA. In each case, the [100] projection is shown on the left and the [001] projection on the right. The positions of the *d6r* units are color coded (red: position A, yellow: position B, blue: position C). From bottom to top: the arrangement of two *d6r* layers and one layer of SDA (in position A), three *d6r* layers, four *d6r* layers with the second layer of SDAs added, five *d6r* layers with three layers of SDA, and six *d6r* layers showing the completion of the large cavity (in position A) and the beginning of the next one (in position B).

mechanism, but also the fact that just two types of stacking faults occur. Twinning occurs when a cavity is capped after three or five (instead of four) *d6r* layers (Figure 6e and f). Modeling calculations indicate that these cavities are likely to contain water in addition to one or two SDAs, respectively. From the DIFFaX simulations, it is apparent that this twinning occurs infrequently, but it must be included to produce a good profile fit. The 3D 8-ring channel system is preserved, no matter what the stacking sequence. No evidence of extended domains of other 6-ring stacking sequences was found in the HRTEM images. The fault layers appear to be isolated ones in an otherwise pure SSZ-52 *d6r* stacking sequence.

With the use of chemical intuition, a remarkable new zeolite, SSZ-52, has been synthesized, and the details of its structure have been unraveled by applying multiple characterization techniques. Its unusually large cavity integrated into a 3D 8-ring channel system makes SSZ-52 a promising new material with considerable potential in the gas conversion and sequestration

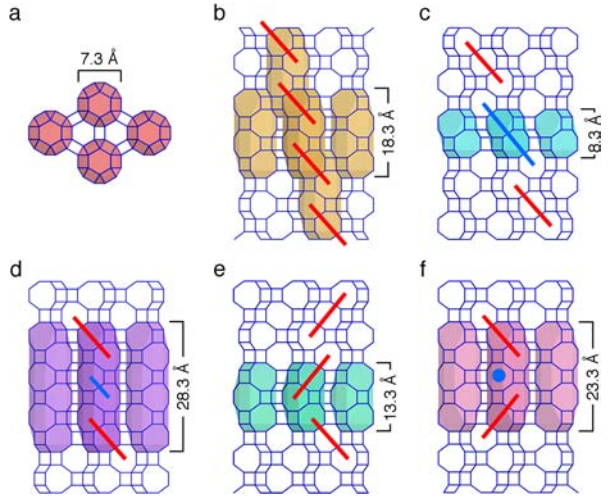

Figure 6. Different types of stacking faults in SSZ-52. (a) The [001] projection showing the arrangement of the cavities highlighted in the [100] projections in c–f. (b) The [100] projection of the ideal ABABCBCAC stacking sequence with four *d6r* layers between the caps of the cavity, (c) the sequence causing the ideal cavity to be halved to form a *cha* cavity (two *d6r* layers), (d) the extension of the ideal cavity by two *d6r* layers, (e) a twinning sequence leading to an *aft* cavity (three *d6r* layers), and (f) a twinning sequence leading to a five *d6r*-layer cavity. The rows of 8-rings seen in the HRTEM images in Figure 3d and Figure S6 in SI are indicated in red, and the stacking faults are highlighted in blue. Approximate free dimensions of the cavities are indicated.

areas that are so much in demand at present as the worlds of energy efficiency and pollution control take center stage.

■ ASSOCIATED CONTENT

Ⓢ Supporting Information

Reaction scheme for the synthesis of the SDA; X-ray powder diffraction patterns for the seven models with nine *d6r* layers; details of the molecular modeling; comparison of the three *d6r* aluminosilicate framework structures; additional TEM information; crystallographic information file for SSZ-52. This material is available free of charge via the Internet at http://pubs.acs.org.

■ AUTHOR INFORMATION

Corresponding Author

mccusker@mat.ethz.ch (L.B.M.); sizo@chevron.com (S.I.Z.)

Notes

The authors declare no competing financial interest.

■ ACKNOWLEDGMENTS

We thank the beamline scientists of the SNBL at the ESRF in Grenoble, France, for their assistance with the powder diffraction measurement, and George Fitzgerald from Accelrys for helpful discussions regarding the use of the Materials Studio software. This work was supported in part by the Swiss National Science Foundation, the Chevron Energy Technology Company, the Swedish Research Council (VR) and the Knut and Alice Wallenberg Foundation through a grant for purchasing the TEM and the project grant 3DEM-NATUR.

■ REFERENCES

(1) Three-letter framework type codes (boldface capital letters) for all zeolites mentioned in the text are given in parentheses.

(2) Baerlocher, Ch.; McCusker, L. B.; Olson, D. H. *Atlas of Zeolite Framework Types*; Elsevier: Amsterdam, 2007; Baerlocher, Ch.; McCusker, L. B. *Database of Zeolite Structures*; http://www.iza-structure.org/databases/.
(3) Jacoby, M. *Chem. Eng. News* **2012**, *90*, 10−16.
(4) Kwak, J. H.; Tran, D. N.; Szanyi, J.; Peden, C. H. F.; Lee, J. H. *Catal. Lett.* **2012**, *142*, 295−301.
(5) Beutel, T. W.; Bull, I.; Moini, A.; Breen, M.; Dieterle, M.; Alerasool, S.; Slawski, B. U.S. Patent Appl. 2011/0165052, 2011.
(6) (a) Korhonen, S. T.; Fickel, D. W.; Lobo, R. F.; Weckhuysen, B. M.; Beale, A. M. *Chem. Commun.* **2011**, 800−802. (b) Fickel, D. W.; Lobo, R. F. *J. Phys. Chem. C* **2010**, *114*, 1633−1640.
(7) An *n*-ring in a zeolite framework structure consists of *n* tetrahedral nodes (e.g., Al, Si, or P) bridged by *n* O atoms. A double 6-ring or *d6r* consists of two 6-rings connected via O atoms to form a hexagonal prism. Composite building units found in more than one framework type have been assigned three letter codes (italic small letters), which are listed in ref 2. Those of interest here are *cha*, *d6r*, and *gme*.
(8) Gies, H.; van Koningsveld, H. *Catalog of Disorder in Zeolite Frameworks*; http://www.iza-structure.org/databases/.
(9) Moliner, M.; Franch, C.; Palomares, E.; Grill, M.; Corma, A. *Chem. Commun.* **2012**, *48*, 8264−8266.
(10) Bull, I.; Muller, U.; Bilge, Y. U.S. Patent Appl. 2012/0208691, 2012.
(11) Lee, G. S.; Zones, S. I. *J. Solid State Chem.* **2002**, *167*, 289−298.
(12) Lee, G. S.; Zones, S. I. U.S. Patent 6,254,849, 2001.
(13) Zones, S. I.; Davis, M. E. *Curr. Opin. Solid State Mater. Sci.* **1996**, *1*, 107−117.
(14) Jackowski, A.; Zones, S. I.; Hwang, S.-J.; Burton, A. W. *J. Am. Chem. Soc.* **2009**, *131*, 1092−1100.
(15) Hudson, M. R.; Queen, W. L.; Mason, J. A.; Fickel, D. W.; Lobo, R. F.; Brown, C. M. *J. Am. Chem. Soc.* **2012**, *134*, 1970−1973.
(16) Baerlocher, Ch.; Hepp, A.; Meier, W. M. *DLS-76. Distance Least Squares Refinement Program*; Institut für Kristallographie: ETH, Zurich, 1977.
(17) *Materials Studio*, 6; Accelrys, Inc.: San Diego, CA, 2012.
(18) Treacy, M. M. J.; Newsam, J. M.; Deem, M. W. *Proc. R. Soc. Lond. A* **1991**, *433*, 499−520.
(19) Corma, A.; Rey, F.; Rius, J.; Sabater, M. J.; Valencia, S. *Nature* **2004**, *431*, 287−290.